International Journal of Biology and Life Sciences
ISSN: 2957-9511 | Vol. 12, No. 3, 2025

Study on the Mechanism of Temperature Rise in Koji Room Fermentation based on the Influence of Microbial Metabolism

Qi Hao [1], Yan Shi [1, 2, *], Zhengquan Yang [3], Chunsong Lin [1], Enhan Wen [1]

[1] School of Mechanical Engineering, Sichuan University of Light Chemical Industry, Yibin Sichuan 644000, China
[2] Sichuan Provincial Key Laboratory of Process Equipment and Control Engineering, Sichuan University of Light Chemical Technology, Yibin Sichuan 644000, China
[3] Sichuan Yibin Minjiang Machinery Manufacturing Co., Ltd., Yibin Sichuan 644000, China

*** Corresponding author:** Yan Shi

Abstract: [Objective] Koji-making rooms are the core loci of solid-state fermentation in Chinese Baijiu production; their hygrothermal state directly governs the kinetics of Daqu fermentation. Empirical retrofits based on artisanal experience no longer satisfy the stringent quality-control and intelligent-design requirements of the modern, highly engineered liquor industry. Here we elucidate the heat-rise balance mechanism that prevails during Daqu fermentation and explicitly incorporate the microbial activity-adaptation response. By quantifying the generation and transport of both heat and moisture throughout the fermentation cycle and regressing an extensive experimental dataset, we developed a steady-state hygrothermal balance model for koji-making room operation. Model predictions of spatial temperature–humidity distributions and substrate-consumption kinetics agreed with measured values within a mean relative error of <5 %, confirming high fidelity to the real system. Subsequent optimisation of ventilation/humidification schedules with the calibrated model revealed that microbial kinetics obey clear environment–activity relationships. For a small-scale koji-making room, an airflow rate of 80 $m^3 h^{-1}$ delivered in five 12-min pulses per hour maximised substrate utilisation efficiency while maintaining thermal equilibrium. These findings underscore the pivotal role of microbial activity adaptation in hygrothermal control and establish, for the first time, a mathematical characterisation of Daqu as both a moisture and a heat source. The model furnishes a quantitative platform for future simulation-based optimisation and offers a new paradigm for the intelligent design of next-generation koji-making rooms.

Keywords: Daqu Fermentation; Koji-making Room; Hygrothermal Balance; Microbial Adaptation; Mathematical Modeling; Intelligent Control.

1. Introduction

Daqu, as the core microbial agent in solid-state Baijiu brewing, directly determines the abundance of flavor precursors in the liquor [1]. During the initial stage of fermentation, the synergistic metabolism of Aspergillus and Saccharomyces cerevisiae provides the basis for the formation of the enzyme system in Daqu [2]. Microorganisms are the core driving force of Daqu fermentation, and their role during the fermentation process is crucial. The traditional Daqu piling fermentation mode relies on manual operation and has a low level of intelligence, which can lead to fluctuations in the growth environment of the Daqu microbial community. The rack Daqu fermentation room, as an improvement to the traditional piling facilities, is more conducive to precise control of environmental parameters and helps promote the standardization and quality improvement of the Daqu production process. However, if the Daqu production process is completely dependent on traditional experience, there are still obvious limitations. Therefore, conducting systematic engineering research has become an urgent problem to be solved at present.

The Chinese Baijiu industry is accelerating its transformation and upgrading: traditional brewing processes are gradually becoming standardized and refined, brewing microorganisms are tending towards intelligent regulation, the integration and innovation of processes are deepening, the aging process is becoming smarter, and the design of liquor bodies is more scientific. These changes have injected new impetus into the industry and pushed the Baijiu industry into a new stage of high-quality development [3].Li Xuan et al. [4], through tracking and detecting the physical and chemical indicators of the liquor mash, found that the changes were significant and closely related to microbial metabolism; Liu Dan et al.[5], through solid-state mixed microbial fermentation under different temperature and humidity conditions, analyzed the changes in microbial community structure and function, indicating that Bacillus subtilis has a perturbing effect on the microbial community structure and metabolism; Xiao Peng et al.[6], by setting two initial fermentation temperatures and combining sequencing and GC-MS technology, found that temperature significantly affects the microbial community succession and flavor substance composition. These studies consistently show that the microbial community structure of Daqu is closely related to the temperature of the Daqu fermentation room.

To promote the mechanization process of Baijiu production, research on the solid-state fermentation process of Daqu has received increasing attention. Huang Haifei [7], through numerical simulation and experiments, studied the humidification process of the Daqu fermentation room, revealing the strong coupling relationship between heat and moisture transfer, providing a basis for the optimization of the Daqu fermentation room structure. Zhou Shuyu et al. utilized a fuzzy neural network to control the temperature and humidity changes in the fermentation environment to meet the uniformity requirements of the internal regions of the Daqu

fermentation room, reducing the reliance on subjective human experience and demonstrating the application potential of intelligent Daqu fermentation rooms. However, the above methods are still mainly based on empirical modifications and lack in-depth exploration of engineering mechanisms, which poses certain difficulties in promotion and application as well as scale expansion. Existing research mainly focuses on the wet and hot factors of the Daqu fermentation room environment. Therefore, establishing a wet and hot model of the Daqu fermentation room to reveal the engineering mechanism of environmental changes and achieve precise control of environmental variables is the key to future optimization.

At present, research on the heat model of the Daqu solid-state fermentation process is still relatively limited. Zhao Yujie et al. [8], based on heat balance, established a biochemical reaction model to explore the impact of Daqu block mass changes on the environment, providing a model basis for the temperature rise mechanism of Daqu fermentation. Other solid-state fermentation forms, such as Han Bing et al. [9], by introducing sub-models of microbial growth, sugar consumption, and product generation, successfully predicted the temperature rise in drum-type dynamic fermentation; there are also related temperature prediction models for packed bed ventilation fermentation, etc. These studies provide solutions to the regulation difficulties of the solid-state fermentation process and offer references for the model construction of Daqu fermentation in the fermentation room.

This study, based on the wet and hot transfer mechanism in the Daqu fermentation room process and combined with the growth and metabolism laws of microorganisms, constructs a wet and hot model of the Daqu fermentation room, analyzes the heat change laws of Daqu fermentation from an engineering perspective, with the aim of providing theoretical basis for the regulation and optimization of Daqu production processes and technical support for the development of intelligent Daqu fermentation rooms.

2. Mathematical Model

2.1. Moisture and Heat Analysis of Koji Fermentation in a Koji Room

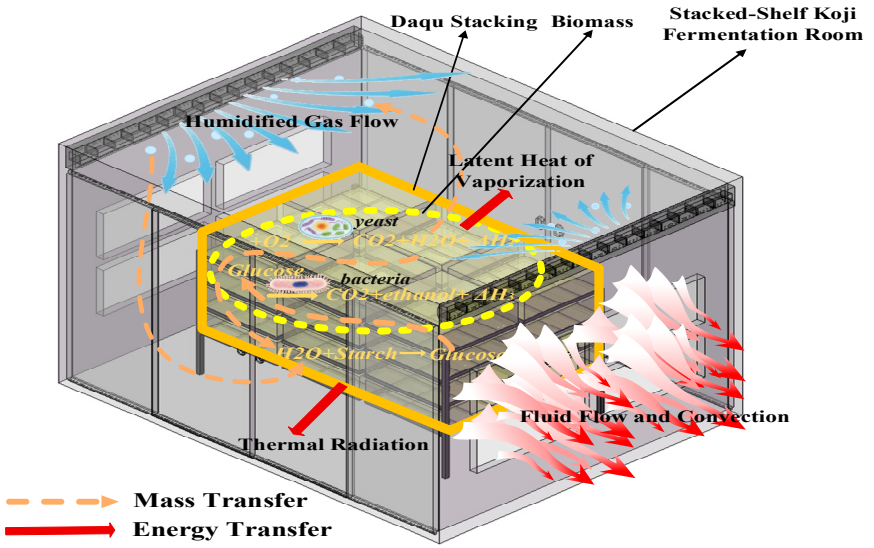

Fig 1. Mechanism of Moisture and Heat Exchange in koji-makingroom

During the natural fermentation process of koji, it exhibits significant moisture generation and heat release characteristics, which can be defined as a biological moisture source and biological internal heat source in the koji room system [10]. As a moisture source, the water in koji includes both bound water and free water. When it evaporates, it absorbs latent heat from the environment to achieve vaporization, and when the gaseous water condenses upon cooling, it releases an equivalent amount of latent heat, forming a periodic "evaporation-condensation" latent heat cycle. This process not only promotes the redistribution of energy within the koji room but also maintains a humidity environment that plays a crucial role in regulating microbial activities: appropriate humidity ensures the normal permeability of cell membranes, promotes the dissolution of nutrients and enzymatic reactions, thereby influencing the microbial community structure and metabolic functions. In terms of heat production, microorganisms continuously generate chemical energy through growth, reproduction, and metabolic processes. Besides meeting their own maintenance needs, the excess energy is released in the form of heat. Due to the inherent low thermal conductivity and limited convection of the solid-state fermentation system, heat tends to accumulate within the material, causing local temperature rises, which further feedback-regulates the succession and metabolic pathways of microorganisms [11]. For the convenience of modeling and analysis, the complex heat-producing biochemical reactions are often simplified into two dominant processes: one is the endothermic starch hydrolysis reaction, and the other is the strongly exothermic microbial growth and metabolic process, which is the main source of net heat production in the system. Heat is mainly transferred through three mechanisms: thermal radiation, thermal conduction, and thermal convection, driving the dynamic changes in the internal temperature distribution of the koji blocks, the thermal state of the air, and the heat exchange in the koji room space. Ultimately, they jointly determine the coupled moisture and heat balance state of the koji room system. The moisture and heat exchange mechanism in the koji room is shown in Figure 1.

2.2. Large-scale Fermentation Reaction

The solid-state fermentation process of large-scale koji can be simplified as the hydrolysis of starch in the koji into sugar

compounds, which are then decomposed into fermentation substances such as ethanol. Research shows that over 70% of the heat involved in the reaction comes from the decomposition of starch and sugar compounds [12]. Therefore, the heat generated by the main heat source in the koji room, the large-scale koji, can be set asΔH_1, ΔH_2 and ΔH_3.

2.2.1. Heat Generation from Starch HydrolysisΔH_1

Wheat, the main raw material in the large-scale koji, has its starch hydrolyzed into sugar compounds during the fermentation process. These sugar compounds then supply the growth and activities of microorganisms. The reaction heat equation for the starch hydrolysis process can be simplified as shown in Equations (1) and (2):

$$(C_6H_{10}O_5)_n(Starch)+nH_2O\xrightarrow{amylase}nC_6H_{12}O_6+\Delta H_1' \quad (1)$$

$$\Delta H_1 = r_{\text{hydro}}(t)\Delta H_1' \quad (2)$$

In the formula: n, the number of glucose monomers in wheat starch; , the reaction heat of starch hydrolysis [13], kJ/kg-starch; $\Delta H_1'$,the heat generated from starch hydrolysis, kJ/h; $r_{hydro}(t)$, the starch hydrolysis rate, kg/h.

2.2.2. Heat Generation from Sugar Compound DecompositionΔH_2, ΔH_3

The dynamic changes of the microbial community during the fermentation process in the koji room affect the changes of sugar compounds in the large-scale koji fermentation process. The main sugar compounds in the large-scale koji fermentation process include glucose, xylose, fructose, and sucrose. Based on the analysis of their content and heat generation, it is known that glucose is the main source of heat-generating substrate [14]. The decomposition of sugar compounds mainly involves aerobic respiration and anaerobic respiration. In the early stage of fermentation, as the temperature in the koji room gradually rises, the growth activity of aerobic bacteria is relatively vigorous, so aerobic respiration mainly occurs during the early fermentation period. In the later stage of fermentation, as the temperature gradually drops and reaches the suitable temperature range for aerobic bacteria, the aerobic bacteria become active again and decompose sugar compounds. The aerobic reaction heat ΔH_2 is shown in Equations (3) to (5):

$$C_6H_{12}O_6+6O_2\xrightarrow{microbial\ metabolism}6CO_2+6H_2O+\Delta H_2' \quad (3)$$

$$\Delta H_2' = \left(\Delta H_G - 6\times\Delta H_{CO_2} - 6\times\Delta H_{H_2O}\right)\times 1000 \quad (4)$$

$$\Delta H_2 = r_{\text{resp}}(t)\Delta H_2' + r_{\text{consume,X2}}(t)\Delta H_2' \quad (5)$$

In the formula: $\Delta H_2'$ is the heat of aerobic microbial metabolic reaction, kJ/kg-glucose; ΔH_G is the combustion enthalpy of glucose, kJ/mol; ΔH_{CO2} is the combustion enthalpy of carbon dioxide, kJ/mol; ΔH_{H2O} is the combustion enthalpy of water, kJ/mol; ΔH_2 is the heat generated from the oxidation and decomposition of sugar compounds, kJ/h;r_{resp} (t) is the glucose consumption rate of facultative aerobic yeast during aerobic respiration, kg/h; $r_{consume,\ X2}$ is the glucose consumption rate of aerobic bacteria during aerobic respiration, kg/h.

During the middle stage of fermentation, the temperature in the fermentation room gradually rises to the peak temperature and remains stable. Due to the high temperature, the activity of aerobic bacteria decreases, and anaerobic bacteria become dominant. During this period, the decomposition of starch and sugar compounds reaches the highest value. Therefore, the anaerobic reaction heat ΔH3 based on the microbial activity consumption rate of glucose can be calculated according to formulas (6) to (8).

$$C_6H_{12}O_6\xrightarrow{Yeast/Bacteria}2C_2H_5OH+2CO_2+\Delta H_3' \quad (6)$$

$$\Delta H_3' = \left(\Delta H_G - 2\times\Delta H_{C_2H_5OH} - 2\times\Delta H_{CO_2}\right)\times 1000 \quad (7)$$

$$\Delta H_3 = r_{\text{ferm}}(t)\Delta H_3' + r_{\text{consume,X3}}(t)\Delta H_3' \quad (8)$$

In the formula: $\Delta H_3'$ is the anaerobic reaction heat of yeast/bacteria, kJ/kg-glucose; ΔH_{C2H5OH} is the combustion enthalpy of ethanol, kJ/mol; ΔH_3 is the heat generated from the oxidation and decomposition of sugar compounds, kJ/h; $r_{ferm}(t)$ is the glucose consumption rate of facultative anaerobic yeast during anaerobic fermentation, kg/h; $r_{consume,\ X3}$ is the glucose consumption rate of anaerobic bacteria during anaerobic fermentation, kg/h.

2.2.3. Heat of Daqu Fermentation ΔH

Through reasonable simplification of the biochemical reactions in the solid-state fermentation of Daqu, the heat of Daqu fermentation is shown in formula (9):

$$\Delta H = \Delta H_1 + \Delta H_2 + \Delta H_3 \quad (9)$$

In the formula: ΔH is the heat of the solid-state fermentation process of Daqu based on the growth activity of the microbial community, kJ/h.

2.3. Substrate Consumption in Daqu

The wet heat mechanism of Daqu mainly relies on the decomposition reactions of substrates, which mainly involve biochemical reactions of microorganisms. The rate of substrate consumption is closely related to the activity of microorganisms. Therefore, the suitability of the wet heat environment is crucial for the biochemical reactions.

2.3.1. Microbial Community Activity Model

The activity of the microbial community during Daqu fermentation has a significant impact on substrate consumption. The activities of aerobic and anaerobic microbial communities vary greatly under different oxygen concentrations, temperatures, and humidity levels. Therefore, the activity of the microbial community is added as a marker for the decomposition of sugar substances during the fermentation cycle [15]. The activity of the microbial community is calculated based on real-time temperature and oxygen concentration. The activity model of aerobic microbial communities is shown in formulas (10) to (12):

$$A_T(T)=\begin{cases}0, & T<20\\ 25+6(T-20), & 20\le T<30\\ 85+1.5(T-30), & 30\le T<40\\ 100-15(T-40), & 40\le T<45\\ 25-5(T-45), & 45\le T<50\\ 0, & T\ge 50\end{cases} \quad (10)$$

$$A_O(O_2)=\begin{cases}0, & O_2<5\\ 20(O_2-5), & 5\le O_2<10\\ 100, & 10\le O_2<15\\ 100-16.67(O_2-15), & 15\le O_2<21\\ 0, & O_2\ge 21\end{cases} \quad (11)$$

$$A_{\text{combined}} = \frac{A_T}{100}\times A_O \quad (12)$$

In the formula: $A_T(T)$ is the activity of aerobic bacteria based on temperature, %; $A_O(O_2)$ is the activity of aerobic

bacteria based on O_2 concentration, %; $A_{combined}$ is the combined activity of aerobic bacteria, %.(1. Note: 20–30℃: +6% per 1℃ increase (rapid increase); 30–40℃: approaching the optimum, +1.5% per 1℃; 40–45℃: beginning to lose activity, -15% per 1℃; 45–50℃: rapid loss of activity, -5% per 1℃; ≤20℃ or ≥50℃: activity loss [16]; 2. Note: <5% O_2: hypoxia, activity is 0; 5–10%: +20% per 1% increase in O_2; 10–15%: optimal plateau zone; 15–21%: high oxygen leads to inhibition (possibly due to excessive evaporation or free radical damage), -16.67% per 1% increase in O_2; ≥21%: activity is zero [17].)

The activity model of anaerobic microbial communities is shown in formulas (13) to (15):

$$AN_T(T)=\begin{cases}10, & T<20\\ 10+6(T-20), & 20\le T<30\\ 70+2(T-30), & 30\le T<40\\ 90-5(T-40), & 40\le T<50\\ 40+6(T-50), & 50\le T<60\\ 100-2(T-60), & 60\le T<70\\ 80, & T\ge 70\end{cases} \quad (13)$$

$$AN_O(O_2)=\begin{cases}100, & O_2<5\\ 100-20(O_2-5), & 5\le O_2<10\\ 0, & O_2\ge 10\end{cases} \quad (14)$$

$$AN_{\text{combined}}=\frac{AN_T}{100}\times AN_O \quad (15)$$

In the formula: $AN_T(T)$ is the activity of anaerobic bacteria based on temperature, %; $AN_T(O_2)$ is the activity of anaerobic bacteria based on O_2 concentration, %; $AN_{combined}$ is the combined activity of anaerobic bacteria, %.

(1.Note:20–30°C: Mesophilic anaerobes activate, increasing by 6% per °C.30–40°C: Activity continues to rise, but the rate of increase slows.40–50°C: Mesophilic species decline, activity decreases.50–60°C: Thermophilic anaerobes take over, increasing by 6% per °C.60–70°C: Activity gradually declines.≥70°C: Activity plateaus at 80% (due to extreme thermophiles) [16].2.Note:<5% O_2 concentration: Strict anaerobic conditions, activity at 100%.5–10% O_2 concentration: Increasing oxygen partial pressure inhibits anaerobic metabolism, decreasing activity by 20% per 1% O_2 concentration.≥10% O_2 concentration: Complete inhibition [17].)

2.3.2. Starch Consumption Rate

At the initial stage of fermentation, starch is only partially hydrolyzed by a small amount of amylase into dextrin, with a reduction typically ranging from 5% to 10% of the initial content. [18] Research on solid-state fermentation of sorghum indicates that the starch loss rate is 38% in the first week, mainly due to the preliminary hydrolysis of exposed starch by amylase. After the 8th day, the starch content drops significantly, and it decreases slowly and fluctuates steadily during the 20-day storage period. [19] As the initial substrate, starch is hydrolyzed into glucose through hydrolysis reactions. The hydrolysis rate is influenced by temperature and is positively correlated with the biomass of yeast. Microorganisms secrete glucoamylase to drive the hydrolysis. Therefore, the starch consumption rate and concentration are calculated by Equations (16) and (17):

$$r_{\text{hydro}}(t)=k_{\text{hydro},s}\times\exp\left(\frac{-E_{\text{a,hydro},s}}{R\times(T(t)+273.15)}\right)\times A(t)\times 10^{X(t)-5}\times f_{\text{RH}} \quad (16)$$

$$A_{\text{total}}(t)=A(t)\times\frac{m_{\text{dry}}(t)}{1000} \quad (17)$$

In the formula: $k_{hydro,s}$ is the starch hydrolysis rate constant in the s-th stage [4]; $E_{a,hydro,s}$ is the activation energy of hydrolysis, J/mol; $A(t)$ is the starch concentration at time t, g/kg-dry starter; $X(t)$ is the yeast biomass, lgCFU/g; R is the gas constant; f_{RH} is the humidity factor; $A_{total}(t)$ is the change in total starch content, kg; $m_{\text{dry}}(t)$ is the dry matter mass of the starter at time t, kg.

2.3.3. Glucose Consumption Rate

The decomposition of glucose relies on the growth and activity of yeast. The growth of the yeast population is regulated by "substrate (glucose) concentration, temperature, and feedback from target biomass". By introducing the parameter of microbial population activity into the modified Monod model, the yeast growth kinetics model is as follows in Equations (18) to (20):

$$\frac{dX(t)}{dt}=[0.035(Y_{xs}r_{\text{resp}}(t)+Y_{xs}r_{\text{ferm}}(t))+0.85k_{\text{growth},s}f_{\text{temp,X}}]\times X(t-1) \quad (18)$$

$$r_{\text{resp}}(t)=f_{\text{resp,active}}\times k_{\text{resp,T}}\times\frac{S(t)\times 10^{X(t)-5}}{K_{\text{sx}}+S(t)}\times A_{\text{combined}} \quad (19)$$

$$r_{\text{ferm}}(t)=f_{\text{fermactive}}k_{\text{ferm,T}}\times\frac{S(t)\times 10^{X(t)-5}}{K_{\text{sp}}+S(t)}\left(1-\frac{P(t)}{P_{\text{max}}}\right)\times AN_{\text{combined}} \quad (20)$$

The instantaneous change rate of yeast biomass, $dX(t)/dt$, is expressed in lgCFU/g·h; Y_{xs} the yield coefficient of yeast biomass [20], is in g/g; kgrowth,s, the inherent empirical growth potential corresponding to the fermentation stage [21]; ftemp,X, the temperature inhibition factor [20]. S(t), the glucose concentration in the dough block at time t, is in g/kg dry dough; P(t), the ethanol concentration at time t, is in g/kg [21]; Pmax, the upper limit of ethanol tolerance, is in g/kg.

The aerobic and anaerobic respiration of the glucose-decomposing bacterial community are equally important. The kinetic models of the activity of the glucose-decomposing bacterial community, the growth rate of the glucose-decomposing bacteria, and the glucose consumption rate based on the Monod model are as follows in Equations (21) to (24):

$$\frac{dX_2(t)}{dt}=[0.09r_{\text{consume,X2}}(t)+0.82k_{\text{X2,s}}f_{\text{temp,X2}}]X2(t-1)-k_{\text{d,X2,s}}X2(t-1) \quad (21)$$

$$\frac{dX_3(t)}{dt}=[0.07r_{\text{consume,X3}}(t)+0.8k_{\text{X3,s}}f_{\text{temp,X3}}]X3(t-1)-k_{\text{d,X3,s}}X3(t-1) \quad (22)$$

$$r_{\text{consume,X2}}(t)=q_{\text{smax,X2}}\times\frac{10^{X2(t-1)-6}S(t)}{K_{\text{s,X2, glu}}+S(t)}A_{\text{combined}} \quad (23)$$

$$r_{\text{consume,X3}}(t)=q_{\text{smax,X3}}\times\frac{10^{X3(t-1)-6}S(t)}{K_{\text{s,X3,glu}}+S(t)}AN_{\text{combined}} \quad (24)$$

In the formulas:$dX_2(t)/dt$,$dX_3(t)/dt$,the instantaneous change rates of aerobic and anaerobic bacteria biomass, lgCFU/g·h; $k_{X2,\,s}$,k_{X3}, the intrinsic growth potential coefficients of aerobic and anaerobic bacteria for glucose decomposition in fermentation stage s;$f_{temp,\,X2}$,$f_{temp,\,X3}$, the temperature inhibition factors of aerobic and anaerobic bacteria; $k_{d,\,X2,\,s}$,$k_{d,\,X3,\,s}$,the death rate constants of aerobic and anaerobic bacteria for glucose decomposition in fermentation stage s;$q_{smax,\,X2}(t)$, $q_{smax,\,X3}(t)$, the maximum consumption rates of aerobic and anaerobic bacteria for glucose, g/(kg dry starter·h);

2.4. Moisture and Heat Balance in the Starter Room

Based on the moisture and heat exchange mechanism shown in Figure 1, the following assumptions are made: the spatial heterogeneity of the starter room is ignored, and the temperature of the starter blocks is calculated based on the temperature at the center of the blocks; the change in the moisture content of the starter blocks is all calculated as evaporation; for the exchange of indoor and outdoor temperature and humidity and the neglect of heat transfer through the walls and floor, all are estimated using air radiation and air flow [8]. Based on the first law of thermodynamics, under the current assumptions, a heat balance model for the starter room system can be established as shown in Equation (25):

$$Q_Q = Q_F - Q_E - Q_J \tag{25}$$

In the formula: Q_Q, the cumulative heat of the starter blocks during the fermentation process, kJ; Q_F, the total heat generated by fermentation during the fermentation process, kJ; Q_E, the latent heat of water evaporation during the fermentation process of the starter, kJ; Q_J, the heat of the indoor air in the starter room and the heat change due to the exchange of moisture and heat between the indoor and outdoor air.

2.4.1. Fermentation Heat Q_F

The heat generated by the fermentation process of the starter as a heat source is provided by the growth activities of the microbial community, as shown in Equation (26):

$$Q_{\mathrm{F}} = \Delta H \times t \tag{26}$$

In the formula: Q_F, the heat of the fermentation reaction, kJ; t, the fermentation time, h.

2.4.2. Evaporation Latent Heat Q_E

High-temperature and medium-temperature starters in solid-state fermentation act as a "moisture source", and microbial respiration and metabolism are important sources of moisture production in starters [22]. The moisture production of starters can be simplified as the respiration reaction, and the latent heat of evaporation can be calculated using Equations (27) and (28):

$$Q_{\mathrm{E}} = \frac{(r_{\mathrm{resp}}(t) + r_{\mathrm{consume,X2}}(t)) \times \alpha \times r \times t}{\mathrm{I}} \tag{27}$$

$$\alpha = \frac{M_G}{6M_{H2O}} \tag{28}$$

In the formulas: r, the latent heat of water evaporation, kJ/kg; α, the relationship between the content changes of glucose and water, kg-glucose/kg-water; M_G, the molar mass of glucose, g/mol; M_{H2O}, the molar mass of water, g/mol; I, the proportion of respiration evaporation latent heat.

2.4.3. Heat of the Air in the Starter Room Q_J

The heat of the indoor air in the starter room mainly consists of two parts: the heat carried by the current mixed moist air in the starter room and the heat carried by the mixed moist air introduced by the humidifier. The current mixed moist air in the starter room is mainly composed of two parts: one is the moist vapor formed due to the latent heat of evaporation, and the other is the original dry air in the starter room. The humidifier operates in an intermittent mode. During the process of regulating the moisture and heat balance in the starter room, the introduction of moist air by the humidifier will cause the original moist air in the starter room to be passively discharged; at the same time, the moist air introduced by the humidifier mixes with the remaining moist air in the starter room to form new mixed moist air, and the heat of this mixed moist air can be calculated based on the thermodynamic parameters of moist air using Equations (29) to (31):

$$Q_J = C_J m_J \Delta T_J \tag{29}$$

$$C_J = \frac{(m_a + m_{ta} - \frac{m_{\mathrm{a}} + m_v}{V_{room}}\dot{V}_{\mathrm{sup}}t)C_a + (m_v + m_{tv} - \frac{m_v}{V_{room}}V_{\mathrm{sup}}t)C_v}{m_J} \tag{30}$$

$$m_J = m_{\mathrm{a}} + m_v + m_{ta} + m_{tv} - \frac{m_{\mathrm{a}} + m_v}{V_{room}}\dot{V}_{\mathrm{sup}} \times t \tag{31}$$

In the formulas: C_J, the specific heat capacity at constant pressure of the mixed gas, kJ/(kg·℃); m_J, the mass of the mixed air, kg;ΔT_J, the temperature change of the mixed air, ℃; m_a, the mass of dry air, kg; m_{ta}, the mass of dry air introduced by the humidifier, kg; V_{room}, the volume of the starter room, m³; $\dot{V}_{\mathrm{sup}}$, the volumetric air flow rate of the humidifier, m³/h; C_a, the specific heat capacity at constant pressure of dry air, kJ/(kg·℃); mv, the mass of moist air, kg; mtv, the mass of moist air, kg; C_v, specific heat capacity of water vapor at constant pressure, kJ/(kg · ℃);

The moisture content of the air with four different humidity levels in the fermentation room varies according to the real-time changes in the temperature of the fermentation room, and the air mass is also different. According to the engineering balance calculation standard, the air mass of each component in the room can be calculated as shown in Equations (32) to (38):

$$m_a = V_{room} \times \rho(T(t)) \tag{32}$$

$$m_{ta}(t) = \rho(T(t))\dot{V}_{\mathrm{sup}} \times t \tag{33}$$

$$m_v = (r_{resp}(t) + r_{consume,X2}(t))\alpha \times t + d(t)m_a \tag{34}$$

$$m_{tv}(t) = d(t)m_{ta}(t) \tag{35}$$

$$\rho(T(t)) = 1.293\frac{273}{T(t) + 273} \tag{36}$$

$$d(t) = 0.622\frac{\phi P_{sat}\left(T(t)\right)}{P_{atm} - \phi P_{sat}\left(T(t)\right)} \tag{37}$$

$$P_{sat}(T) = 0.61094 \cdot \exp\left(\frac{17.625\left(T(t)\right)}{\left(T(t)\right) + 243.04}\right) \tag{38}$$

In the formulas: ρ(T(t)), dry air density at the current time's temperature (linear error < 1% within the range of 20–60°C in the formula engineering simplification), kg/m³; d(t), moisture content, kg water vapor/kg dry air; $P_{sat}(T)$, saturated water vapor pressure corresponding to temperature T°C (using Magnus formula with error < 0.2% within -30~70°C), kPa; Patm, local atmospheric pressure, 101.325 kPa.

2.4.4. Heat of the Fermentation Block Q_Q

The heat of the fermentation block is calculated based on the temperature change of the fermentation block and the specific heat capacity. The quality of the fermentation block can be estimated based on the microbial activity of the Daqu as shown in Equations (39) to (40):

$$Q_Q = C_Q m_Q \Delta T_Q \tag{39}$$

$$m_Q = \left[m_{dry,0} - \int_0^t r_{hydro}d\tau - (1.467\left[\int_0^t \left[r_{resp} + r_{consume,X2}\right]d\tau + \int_0^t \left[r_{ferm} + r_{consume,X3}\right]d\tau\right) + \right.$$

$$Y_{xs}\int_0^t[r_{resp}(\tau)+r_{ferm}(\tau)]d\tau+Y_{x2}\int_0^t r_{consume,X2}(\tau)d\tau+Y_{x3}\int_0^t r_{consume,X3}(\tau)d\tau]+$$
$$\left[m_{water,0}+0.6\int_0^t[r_{resp}(\tau)+r_{consume,X2}(\tau)]d\tau-\frac{(r_{resp}+r_{consume,X2})\alpha t}{I}\right] \quad (40)$$

In the formulas: C_Q, specific heat capacity of the starter block, kJ/(kg · ℃); m_Q, mass of the starter block, kg; ΔT_Q, temperature change of the starter block, °C; $m_{dry,0}$, initial dry starter mass, kg; $m_{water,\ 0}$, initial water content of the starter block, kg.

2.4.5. Temperature of the Starter

According to the principle of heat and moisture balance, the remaining heat after the starter generates and loses heat maintains the temperature of the starter. Therefore, the starter temperature model can be derived from equation (39) as shown in equation (41):

$$T_{Q,i}=T_{Q,i-1}+\frac{\Delta Ht-\frac{(r_{resp}(t)+r_{consume,X2}(t))\alpha rt}{I}-C_J m_J\Delta T_J}{C_{P,Q}m_Q} \quad (41)$$

3. Model Construction and Data Analysis

The mathematical model of the starter room in Chapter 1 was built using the MATLAB platform and parameters related to the starter fermentation process were added. Through data collection and comparison with experimental data from literature, the actual fermentation environment of the starter room was simulated.

3.1. Verification of Biomass Reaction in Aspen Plus

The verification of the microbial growth reaction in the previous text was carried out by using the professional biomass fermentation function in the Aspen Plus platform to simulate the changes in starch, glucose, and microbial content.

3.1.1. Establishment of Biomass Reaction

Based on Chapter 1.2, the reaction components involved in the biochemical reactions of the starter are listed in Table 1. The starch reaction and glucose decomposition reaction are simplified to occur in the batch reactor as shown in Figure (2). The biomass communities DCM and PROTEIN represent the glucose-decomposing community and the community generated by microbial growth, respectively. The batch reactor was used mainly considering the continuous exchange of air flow with the outside environment during the starter room fermentation process and the intermittent feeding of the starter. The fermentation cycle is 30 days, then the starter.

Table 1. Reaction components

Name	Attributes
GLC (C6H12O6)	Glucose
C6H10O5	Starch
C2H5OH	Ethanol
NH4SO4	Nitrogen source
DCM	Biomass microbial community
PROTEIN	Biomass microbial community
H2O	Conventional components
CO2	Conventional components
N2	Conventional components
O2	Conventional components

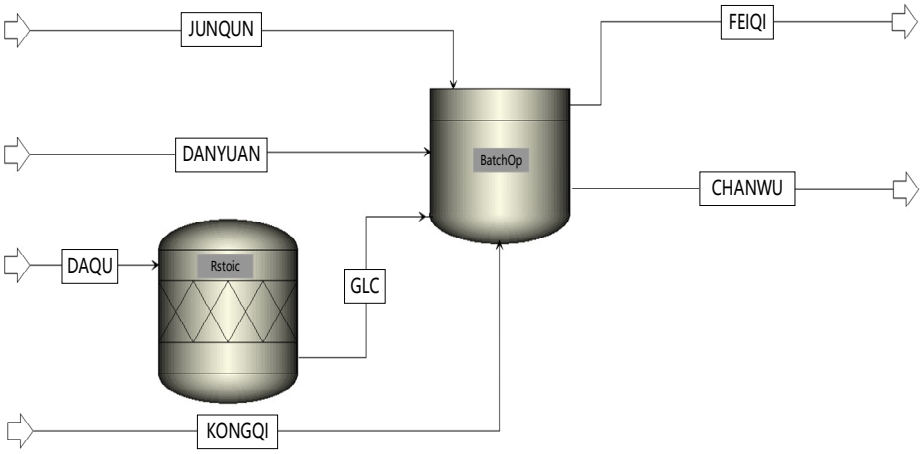

Fig 2. Flowchart of Daqu Fermentation Intermittent Reaction Process

The incorporation of the Monod-Moser model into the biomass reactions introduces a kinetic exponent α, enabling flexible adaptation to the regulatory effect of glucose concentration on microbial metabolic rates. At low glucose concentrations, $S^{\alpha}\approx S$ (if α=1), and the metabolic rate increases linearly with substrate concentration. As the concentration approaches the saturation constantK_S, the rate growth slows and gradually reaches saturation. By integrating microbial mortality rates, relevant growth parameters for the microbial community can be derived.

Aligning with the actual fluctuations in glucose concentration during Daqu fermentation (such as the dynamic balance of substrate concentration during the mid-term peak temperature phase), this model accurately captures the kinetics of microbial glucose utilization. It provides a reliable foundation for quantifying subsequent microbial growth and substrate consumption rates. The Monod-Moser model is expressed as Equation (42):

$$\frac{dX(t)}{dt}=Y_{xs}\cdot\left(\frac{S(t)^{\alpha}}{K_{S,X}+S(t)^{\alpha}}\right)\cdot k_{growth,s}\cdot f_{temp,X}\cdot\left(1-\frac{P(t)}{P_{\max}}\right) \quad (42)$$

3.1.2. Biomass Reaction Analysis

Based on the Monod-Moser model, the kinetic model of yeast growth can be extended to incorporate substrate response. Meanwhile, the metabolic rates of glucose-decomposing microbial communities (aerobic and anaerobic) are also linked to substrate concentrations through this model, achieving a coupled description of "substrate–microbial community–metabolism," as illustrated in the fermentation

liquid retention chart below:

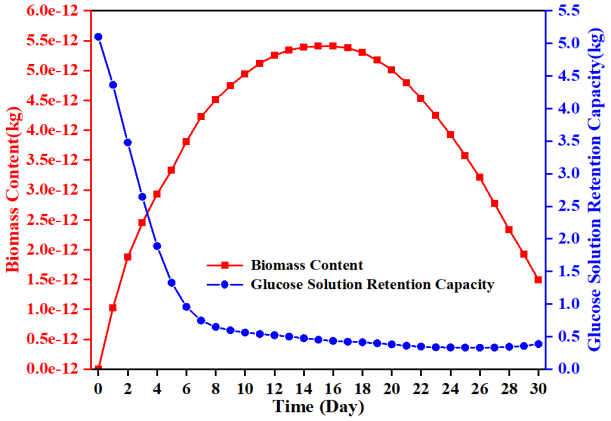

Fig 3. Fermentation Liquid Retention Chart

From Fig. (3), it can be observed that during the initial fermentation stage, continuous feeding leads to a rapid increase in glucose content and a surge in microbial population. In the mid-fermentation stage, glucose content begins to decline. As starch continues to decompose and the microbial decomposition rate of glucose reaches equilibrium, the glucose retention stabilizes at around 0.5 kg. The starch retention eventually remains at 500 kg, indicating that the starch fermentation reaction has reached over 80% completion by the end of fermentation.

In summary, the biomass reactions based on the Aspen Plus platform validate the impact of incorporating the Monod model on Daqu fermentation, providing a basis for subsequent modeling of temperature and humidity in the fermentation room using MATLAB.

3.2. MATLAB Fermentation Process Parameter Analysis

The MATLAB platform was used to construct the mathematical model of temperature and humidity coupling in the fermentation room proposed in Chapter 1. Parameters of the Daqu fermentation process (such as microbial metabolic heat value and initial substrate concentration) from Table 1 were embedded into the model. By comparing simulated data (e.g., fermentation room temperature, substrate content) with experimental data from references [19, 24], the actual fermentation environment was fitted, providing a reliable model foundation for subsequent fermentation process analysis and parameter regulation.

To meet the requirements for high-quality fermentation of Daqu in box-style shelf fermentation rooms, key parameters of the fermentation process must first be identified to support model inputs. The complete fermentation cycle of Daqu is 30 days. Parameters related to the fermentation room and fermentation process are provided in Table 2, serving as core inputs for the subsequent mathematical model of the fermentation room and ensuring the simulation closely aligns with the actual fermentation environment:

Table 2. Relevant parameters of Daqu fermentation process

Initial Parameters	Parameter Values
Number of Qu Blocks	576 blocks
Qu Block Dimensions	310mm×200mm×52mm
Fermentation Room Volume	15m^3
Initial Mass of Qu Block	6kg
Initial Moisture Content	45%

Based on the constructed fermentation room model, the three key indicators of the fermentation process—"temperature change, heat drive, and substrate consumption"—were analyzed to validate the consistency between the model and actual fermentation patterns.

3.2.1. Analysis of Temperature Variation in Fermentation Room

The simulation results of this model were compared with experimental data from the literature, as shown in Fig. (4). The dynamic temperature trend of Daqu exhibits significant consistency with the environmental temperature changes in the fermentation room.

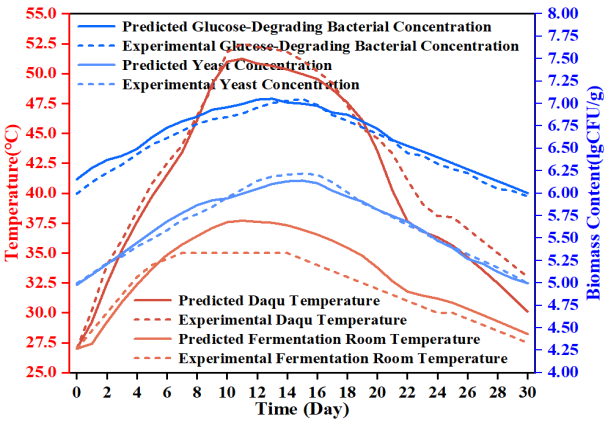

Fig 4. Curves of temperature and biomass varying with fermentation time

During the initial fermentation stage (0–8 days), the Daqu temperature rapidly increased starting from an initial 26°C. In this stage, yeast and glucose-decomposing bacteria simultaneously entered the logarithmic growth phase. Microbial activity monitoring indicated that aerobic communities (dominated by Bacillus and Aspergillus) exhibited high activity. Starch-based substrates were rapidly hydrolyzed, generating large amounts of glucose, providing ample carbon sources for microbial metabolism. The high heat value of aerobic respiration (15,572 kJ/kg) made this metabolic process the core driver of the rapid temperature rise in the fermentation room and Daqu.

During the mid-fermentation stage (8–17 days), the Daqu temperature gradually increased to around 51°C and entered a plateau phase. High temperatures and limited oxygen supply inhibited the activity of aerobic communities, while anaerobic microorganisms (primarily Lactobacillus) entered a metabolically active phase. Although the heat value of anaerobic respiration was lower (389 kJ/kg), the accumulated glucose, continuous starch hydrolysis, and peak microbial biomass collectively maintained the stability of the plateau temperature [23].

In the late fermentation stage (17–30 days), as starch substrates were continuously consumed, the starch hydrolysis rate gradually decreased according to the substrate concentration regulation mechanism of the Monod model. Prolonged high-temperature stress led to the decline of some microorganisms, with anaerobic activity weakening due to heat stress, while aerobic activity showed periodic recovery. Although the metabolic heat values of both communities remained high, insufficient substrate supply caused an overall decline in metabolic rates. Simultaneously, heat dissipation through water evaporation and perforated plate mechanisms in the fermentation room promoted a gradual return of the environmental and Daqu temperatures to initial levels. The

entire fermentation process reflects the dynamic balance between microbial heat production and fermentation room heat dissipation, revealing the self-regulating characteristics of the Daqu fermentation system.

3.2.2. Heat Analysis Driven by Microbial Activity

The trends in microbial activity calculated using Equations (10)– (15) are shown in Fig. (5). The activity of aerobic and anaerobic communities was significantly influenced by environmental changes, exhibiting distinct variations.

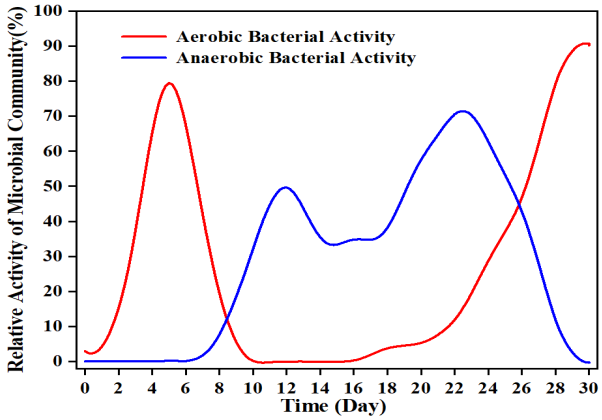

Fig 5. Changing trend of microbial community activity

The simulation results of parameter calculations based on Equations (9) and (39) are shown in Fig. (6). The dynamic changes in the heat of the Qu blocks (Q_Q) are highly coupled with the Daqu temperature process, clearly revealing the heat-driven mechanisms at different fermentation stages:

In the first 10 days, Q_Q rose rapidly, corresponding to the rapid temperature increase phase of Daqu. During this stage, cumulative heat from aerobic respiration and fermentation hydrolysis served as the core driving force. The active metabolism of aerobic microorganisms (e.g., molds, aerobic bacteria) and the hydrolysis of substrates such as starch synergistically released heat, driving the temperature up quickly.

From 10 to 20 days, Q_Q oscillated near the zero mark, aligning with the "mid-plateau" characteristic of Daqu temperature. Anaerobic communities were active, and fermentation heat became the main source of heat production. However, the latent heat of water evaporation. (Q_E) significantly increased under high temperatures, removing large amounts of heat. This created a dynamic balance between anaerobic heat production and evaporative heat dissipation, maintaining stable heat levels.

After 20 days, fell below the zero mark, and Daqu temperature subsequently declined. Although aerobic activity increased and anaerobic activity slowed, metabolic heat production sharply decreased due to substrate scarcity. The heat exchange with fermentation room air (Q_J, associated with ventilation and humidifier operation) became the dominant factor in heat changes. The continued enhancement of ventilation-driven heat dissipation eventually led to a sustained decrease in fermentation room temperature. Combined with the high agreement between the earlier temperature rise predictions and experiments, the correctness of the fermentation room temperature model is preliminarily verified.

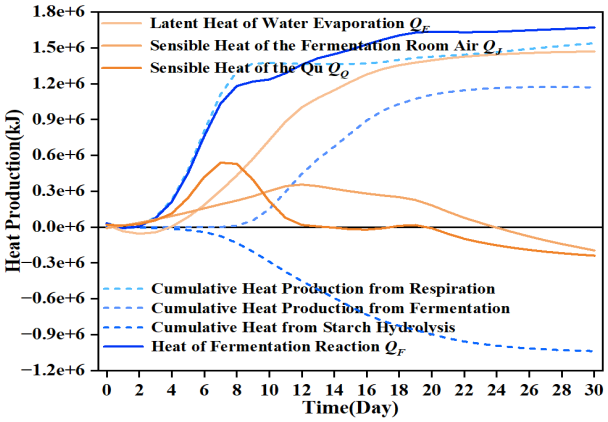

Fig 6. Curve of heat variation

3.2.3. Analysis of Substrate Consumption in Daqu

The initial substrates in Daqu are primarily starch and small amounts of sugar compounds.

As shown in Fig. (7), the starch content showed a slight increasing trend in the first 10 days of fermentation. This may be due to the suitable temperature in the fermentation room for aerobic community growth and the high initial glucose content in Daqu. The abundant energy produced by aerobic decomposition and metabolism provided sufficient conditions for the reproduction of other microbial communities, while starch utilization was low in this stage, leading to an increased proportion of starch in the Qu medium. The simulation data from the biological model showed high consistency with the results from reference [19], though the simulated starch content was generally higher than the literature data. This discrepancy may be because the model did not include some starch-decomposing communities. However, the overall error was less than 5%, validating the correctness of the starch-decomposing community model.

As fermentation temperature gradually increased, the starch decomposition rate accelerated, producing large amounts of glucose. As shown in Fig. (4), the proliferation of glucose-decomposing communities prompted rapid decomposition of the generated glucose, causing glucose concentration to drop and remain at low levels with fluctuations. Around days 12–18, glucose concentration fluctuations were significant, likely due to reduced activity of some glucose-decomposing communities under high temperatures during the plateau phase. These fluctuation characteristics align well with glucose concentration changes reported in references [14,24], with fluctuation amplitudes within a 5% error range, validating the correctness of the glucose-decomposing community model.

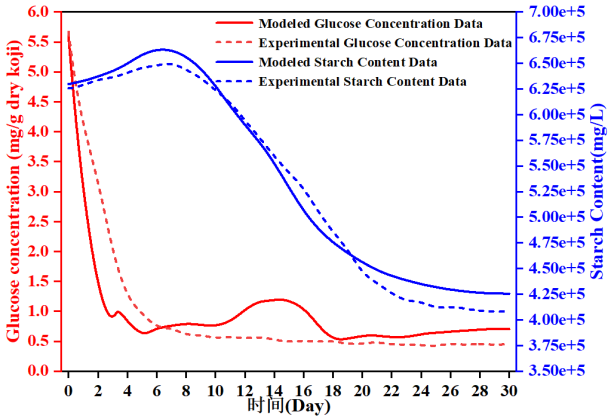

Fig 7. Changing trend of substrate content

3.2.4. Model Parameter Regulation

Based on the microbial-driven coupled temperature and humidity model of the fermentation room, Equation (29) was used to regulate temperature and humidity inside the fermentation room. Fig. (8) shows the dynamic changes in temperature under different combinations of ventilation frequency and ventilation volume during fermentation. These patterns are highly coupled with microbial community activity and the metabolic processes of starch and glucose.

All experimental groups exhibited the typical Daqu fermentation characteristics of "initial temperature rise—mid-term plateau—late temperature decline," resulting from the sequential proliferation and metabolism of microorganisms such as molds, Bacillus, and yeast, dynamically balanced with ventilation-driven heat dissipation in the fermentation room.

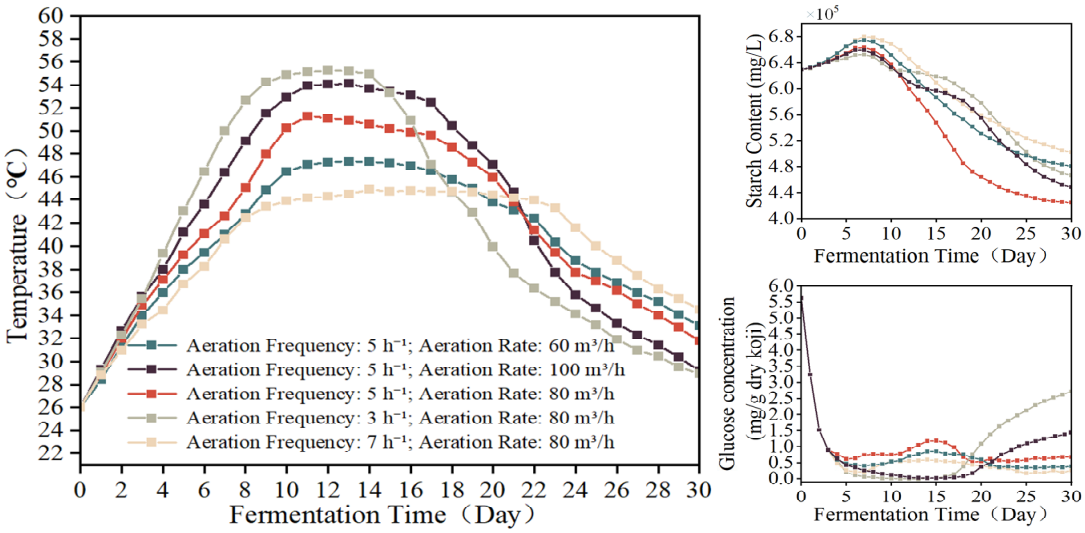

Fig 8. Effects of ventilation frequency and ventilation volume on the koji-making room

From the perspective of ventilation parameter regulation, when the ventilation volume was fixed at 80 m³/h, ventilation frequency directly governed the microbial metabolic rhythm:

At a ventilation frequency of 3 times/h, Daqu temperature rose sharply in the early stage (reaching ~56°C by day 10), exceeding the optimal metabolic temperature range for *Bacillus* (45–55°C). This led to rapid loss of community activity, hindered synthesis of starch-decomposing enzymes (e.g., α-amylase), a sharp decline in starch consumption in the later stage, accumulation of glucose, and insufficient ethanol production [25]. The mid-term plateau was very short, and temperature dropped rapidly in the later stage, indicating nearly stagnant microbial metabolism.

At a ventilation frequency of 5 times/h, the temperature rose gradually to the optimal range for molds (35–40°C) in the early stage, ensuring vigorous mold activity for the initial conversion of starch to glucose. The mid-term plateau stabilized at 52°C (the optimal range for *Bacillus*), promoting extensive reproduction of *Bacillus* and efficient secretion of amylase. Starch consumption peaked, and glucose was rapidly metabolized into ethanol by yeast. The peak community activity lasted about 6 days. During the slow temperature decline in the later stage, yeast remained active, enabling more complete substrate consumption and product formation.

At a ventilation frequency of 7 times/h, the slow temperature rise in the early stage (reaching only ~46°C by day 15) inhibited mold proliferation and initial starch decomposition. The lower mid-term plateau temperature led to insufficient *Bacillus* activity, reduced amylase synthesis, and low levels of starch decomposition and glucose consumption, prolonging the fermentation cycle.

When the ventilation frequency was fixed at 5 times/h, ventilation volume affected metabolic progress by regulating heat and moisture exchange efficiency:

At a ventilation volume of 60 m³/h, insufficient heat and moisture exchange led to elevated humidity in the fermentation room, inhibiting *Bacillus* activity. Starch decomposition and glucose metabolism efficiency were lower than in the medium ventilation volume group, with a short plateau duration and rapid decline in community activity in the later stage.

At a ventilation volume of 100 m³/h, although starch decomposition was faster in the early stage, the mid-term plateau temperature approached the upper tolerance limit for *Bacillus* (55°C), leading to gradual decline in community activity, inhibited amylase synthesis, and reduced glucose consumption rates. Premicrobial decline in the later stage resulted in increased residual substrates, compromising fermentation completeness compared to the medium ventilation volume group of 80 m³/h.

In conclusion, the parameter combination of "ventilation frequency 5 times/h, ventilation volume 80 m³/h" can match the succession rhythm of microbial communities through temperature and humidity regulation, ensuring efficient starch decomposition and orderly conversion of glucose to ethanol, better meeting the process requirements of Daqu fermentation.

4. Conclusion

By combining the model of the fermentation room with microbial activity research equations, this study introduced the Monod substrate consumption model and proposed a microbial activity-based regulation model for the fermentation room. The parameterization error of this model is less than 5% of experimental values, effectively verifying its reliability. From an engineering perspective, the heat changes during Daqu fermentation were analyzed, clarifying the dual attributes of Daqu as both a moisture source and a heat source. By studying humidification and ventilation parameters significantly affecting air heat, it was found that their regulatory role directly influences the degree of Daqu

fermentation and indirectly affects the utilization efficiency of Daqu substrates by altering microbial activity. This study systematically investigated the heating mechanism of Daqu from the perspective of microbial activity and how to maintain suitable microbial activity through environmental regulation, providing theoretical support for the subsequent construction of intelligent models for fermentation rooms.

References

[1] Wu Cheng, Cheng Pingyan, Xie Dan, et al. Correlation analysis among physicochemical factors, flavor compounds and microbial community during the fourth-round pile fermentation of sauce-flavor Baijiu[J]. Food Science, 2023, 44(2): 240-247.

[2] Xu Qianhui, Rao Jiaquan, Zou Yongfang, et al. Succession of microbial community and variation mechanism of metabolites during storage of strong-flavor Daqu[J]. Food Science, 2023, 44(22): 225-234.

[3] Wang Bowen, Wu Qun, Xu Yan, et al. Research progress and trends of microbiome in Chinese Baijiu fermentation starters[J]. Microbiology China, 2021, 48(5): 1737-1746.

[4] Li Xuan, Qi Jusheng, Han Sihai, et al. Variation of physicochemical indices during fermentation of strong-flavor Baijiu Dukang fermented grains[J]. Food and Fermentation Industries, 2019, 45(11): 52-57.

[5] Liu Dan, Chen Jie, Luo Huibo, et al. Perturbation effect of Bacillus subtilis in strong-flavor Daqu on solid-state mixed-culture fermentation system[J]. Food and Fermentation Industries, 2021, 47(11): 38-44.

[6] Xiao Peng, Gao Lu, Li Youming, et al. Effect of temperature on microbial community and flavor compounds during fermentation of light-flavor Baijiu[J]. Food Science, 2025, 46(14): 16-24.

[7] Huang Haifei. Study on humidity numerical simulation and humidification control characteristics in fermentation Qu room[D]. Zigong: Sichuan University of Science & Engineering, 2021.

[8] Zhao Yujie, Jin Guangyuan, Tang Qunyong, et al. Study on the heating mechanism of Daqu fermentation based on heat balance model[J]. Food and Fermentation Industries, 2024, 50(14): 18-25.

[9] Han Bing, Wang Li, Li Shizhong, et al. Advanced solid-state fermentation (ASSF) for ethanol production from sweet sorghum[J]. Chinese Journal of Biotechnology, 2010, 26(7): 966-973.

[10] Yao Y, Luo Y, Wu M, et al. Contribution of moisture to functional microbial succession and functional expression in medium-high temperature Daqu[J]. Food Bioscience, 2025, 69: 106831.

[11] Xiao C, Lu Z M, Zhang X J, et al. Bio-heat is a key environmental driver shaping the microbial community of medium-temperature daqu[J]. Applied and Environmental Microbiology, 2017, 83(23): e01550-17.

[12] González-Hernández Y, Michiels E, Perré P. Heat of reaction in individual metabolic pathways of yeast determined by mechanistic modeling in an insulated bioreactor[J]. Biotechnology for Biofuels and Bioproducts, 2024, 17(1): 137.

[13] Acosta Pavas J C, Alzate Blandón L, Ruiz Colorado Á A. Enzymatic hydrolysis of wheat starch for glucose syrup production[J]. Dyna, 2020, 87(214): 173-182.

[14] Zhou Huixian, Xiong Qinqin, Liu Zhiyong, et al. Dynamic changes of nutritional components in wheat grains during medium-high temperature Daqu fermentation[J]. Food and Fermentation Industries, 2024, 50(15): 48-55.

[15] Ma S, Luo H, Zhao D, et al. Environmental factors and interactions among microorganisms drive microbial community succession during fermentation of nongxiangxing daqu[J]. Bioresource Technology, 2022, 345: 126549.

[16] Anandarajah K, Schowen K B, Schowen R L. Isotope effects and temperature dependences in the action of the glucose dehydrogenase of the mesophilic bacterium bacillus megaterium[J]. Journal of Physical Organic Chemistry, 2013, 26(12): 1066-1070.

[17] Singh S P, Modi D R, Tiwari R K. Biochemical, Thermodynamic and Kinetic Characterization of Glucose Oxidase Purified from Pseudomonas and Actinomyces spp. from Natural Sources[J]. Journal of Pure and Applied Microbiology, 2019, 13(4): 2445-2460.

[18] Qiu F, Li W, Chen X, et al. Targeted microbial collaboration to enhance key flavor metabolites by inoculating Clostridium tyrobutyricum and Saccharomyces cerevisiae in the strong-flavor Baijiu simulated fermentation system[J]. Food Research International, 2024, 190: 114647.

[19] Luo Huibo, Li Danyu, Yang Xiaodong, et al. Determination of starch content changes and patterns during strong-flavor Daqu preparation by continuous flow method[J]. Modern Food Science and Technology, 2013, 29(3): 625-628, 575.

[20] Xu Yan, et al. Modern Baijiu Brewing Microbiology[M]. Beijing: Science Press, 2019.

[21] Li Dahe, et al. Strong-Flavor Baijiu Qu-Making Technology[M]. Beijing: China Light Industry Press, 2023.

[22] Liu W H, Chai L J, Wang H M, et al. Bacteria and filamentous fungi running a relay race in daqu fermentation enable macromolecular degradation and flavor substance formation[J]. International journal of food microbiology, 2023, 390: 110118.

[23] Peng Q, Zheng H, Yu H, et al. Environmental factors drive the succession of microbial community structure during wheat qu fermentation[J]. Food Bioscience, 2023, 56: 103169.

[24] Li Xuan, Qi Jusheng, Han Sihai, et al. Variation of physicochemical indices during fermentation of strong-flavor Baijiu Dukang fermented grains[J]. Food and Fermentation Industries, 2019, 45(11): 52-57.

[25] Yang Y, Niu M S, Yu H, et al. Exploring the contribution of temperature-adapted microbiota to enzyme profile of saccharification in daqu using metagenomics and metaproteomics [J]. LWT, 2024, 197: 115916.